ADMET & DMPK **14** (2026) 3729; *doi: https://doi.org/10.5599/admet.3729*

ADMET

Open Access : ISSN : 1848-7718

http://www.pub.iapchem.org/ojs/index.php/admet

Original scientific paper

Ti_3C_2TX MXene nanosheets/α-MnO_2 nanorods composite-modified electrode for efficient electrochemical determination of dasatinib

Somayeh Tajik[1,*], Razieh Moghimian[1], Fariba Garkani Nejad[2], Fatemeh Sharifi[1], Azadeh Lohrasbi-Nejad[3] and Hadi Beitollahi[2]

[1]*Research Center of Tropical and Infectious Diseases, Kerman University of Medical Sciences, Kerman, Iran*
[2]*Environment Department, Institute of Science and High Technology and Environmental Sciences, Graduate University of Advanced Technology, Kerman, Iran*
[3]*Research and Technology Institute of Plant Production (RTIP), Afzalipour Research Institute (ARI), Shahid Bahonar University of Kerman, Kerman, Iran*

Corresponding Author: E-mail: *tajik_s1365@yahoo.com*

Received: September 9, 2026; Revised: October 30, 2026; Published: November 4, 2026

Abstract

Background and purpose: Chemotherapy is a cornerstone of cancer treatment that utilizes one or more cytotoxic agents to inhibit the growth and proliferation of malignant cells. However, the considerable toxicity and dose-dependent side effects of chemotherapeutic drugs underscore the need for their precise and ultrasensitive quantification. **Experimental approach:** A sensitive, simple, and fast electrochemical method was developed for the determination of dasatinib, utilizing a disposable carbon screen-printed electrode (CSPE) modified with a $Ti_3C_2T_X$ MXene nanosheets (NSs)/α-MnO_2 nanorods (NRs) composite. **Key results:** The utilization of the $Ti_3C_2T_X$ MXene NSs/α-MnO_2 NRs composite on the CSPE surface demonstrated outstanding cyclic voltammetric response. This modification significantly increased the peak current for dasatinib oxidation, from 2.8 µA at the bare CSPE to 11.1 µA at the $Ti_3C_2T_X$ MXene NSs/α-MnO_2 NRs/SPCE surface. Moreover, the oxidation of dasatinib shifted noticeably toward lower potentials on the modified CSPE surface, indicating faster electron-transfer kinetics. The differential pulse voltammetry method was applied for the quantitative determination of dasatinib, achieving a linear response over the concentration range of 0.01 to 400.0 µM with a detection limit of 0.005 µM. Finally, the method's applicability was evaluated for the determination of dasatinib in the tablet sample. Recovery values in the range of 96.6 to 103.8 % were achieved, showing adequate accuracy. **Conclusion:** This analytical approach provides an effective tool for analysing pharmaceutical formulations with potential applications in cancer therapy.

©2026 by the authors. This article is an open-access article distributed under the terms and conditions of the Creative Commons Attribution license (http://creativecommons.org/licenses/by/4.0/).

Keywords

Cancer; electrochemical sensor; screen-printed electrode; two-dimensional transition-metal carbides; nanostructured transition-metal oxides

Introduction

Cancer remains one of the most formidable challenges to global health and one of the leading causes of death worldwide, highlighting the ever-growing need for effective therapies against various types of malignancies [1]. Chemotherapy, a primary strategy of cancer treatment, involves the use of cytotoxic drugs to inhibit the growth of cancer cells [2]. However, these therapeutic agents are often associated with significant side

effects and varying degrees of efficacy, especially when administered in high doses over extended periods [3]. A critical aspect of chemotherapy is the monitoring of drug levels in both pharmaceutical formulations and biological fluids, which helps to optimize dosing, ensure treatment efficacy, and minimize adverse effects. Dasatinib is an orally administered tyrosine kinase inhibitor (TKI) with broad inhibitory activity that has emerged as a key therapeutic agent in the treatment of chronic myeloid leukaemia (CML), particularly in patients who develop resistance or intolerance to imatinib [4-6]. By selectively targeting dysregulated intracellular kinases involved in cell proliferation, survival, and signal transduction, most notably the Abelson tyrosine kinase (ABL), dasatinib interferes with oncogenic signalling pathways that are essential for the maintenance and expansion of leukemic cell populations [7,8]. Its ability to inhibit multiple kinase-dependent pathways contributes to effective suppression of malignant cell growth and improved clinical responses when first-line therapy is unsuccessful. Nevertheless, the broad kinase inhibition profile of dasatinib is associated with several clinically relevant adverse effects, including diarrhoea, peripheral oedema, gastrointestinal bleeding, nausea, fatigue, pyrexia, and headache, which may restrict dose escalation or compromise treatment tolerability [9]. Therefore, accurate quantification of dasatinib in tablet formulations is essential for quality control, ensuring dosage consistency, and maintaining the intended therapeutic potency of the pharmaceutical product. Several analytical methods have been reported for determining dasatinib, including chromatography [10,11], colorimetry [12], spectrophotometry [13], capillary electrophoresis [14], and enzyme-linked immunosorbent assay (ELISA) [15]. Although some of these methods provide high sensitivity and selectivity, they are inherently limited by their reliance on complex and centralized laboratory equipment, long analysis times, high operational costs, and the need for specialized technical expertise. Consequently, these approaches are unsuitable for timely, point-of-care analysis or routine monitoring. To overcome these limitations, electrochemical sensing technology has emerged as a promising solution, offering portability, rapid response, low fabrication cost, and the potential for miniaturization and integration [16-19].

The electrode material fundamentally governs sensor performance and reliability, as it directly influences key factors such as electron-transfer efficiency, electrochemical stability, and selectivity toward the target analyte [20-22]. The choice of electrode material also impacts the sensitivity and response time of the sensor, with materials offering high conductivity and excellent catalytic properties typically leading to improved sensor performance [23,24].

Therefore, selecting the suitable electrode material is crucial for optimizing the sensor's overall efficiency, long-term stability, and practical applicability in real-world settings. Over the past several decades, nano-technology has driven significant progress by enabling precise manipulation of materials at the nanoscale. This advancement allows for the creation of materials and structures with unique physical, chemical, and mechanical properties that are unattainable in their bulk forms, leading to applications in various fields [25].

In particular, recent studies have demonstrated that integrating nanotechnology into electrochemical sensors provides new and effective strategies to enhance their performance. This integration allows for the development of nanomaterial based-modified electrodes, which exhibit superior electrochemical properties, including high surface area, improved conductivity, and increased catalytic activity [26-28].

Consequently, the improved performance of nanostructured materials-based electrochemical sensors positions them as highly attractive tools for medical diagnosis, environmental monitoring, and real-time sensing [29-31].

Metal oxide nanomaterials have attracted significant attention in electrochemical applications due to their versatile properties, including high surface area, tuneable electronic structure, chemical stability, and relatively simple synthesis methods [32]. Among them, manganese dioxide (MnO_2) has gained considerable

(cc) BY

attention as an electrode material due to its good electrochemical properties, cost-effectiveness, and environmentally friendly nature [33]. It's simple synthesis method and high availability make it an attractive choice for various applications. Recently, MnO_2 nanomaterials have shown great promise in fields such as batteries, supercapacitors, solar cells, and electrocatalytic reactions, owing to their ability to be easily modified into different morphologies and structures [34]. The electrochemical behaviour of MnO_2 varies significantly with changes in its morphology, with distinct forms demonstrating enhanced performance. However, the low conductivity of MnO_2 can lead to insufficient utilization of the active material and a decrease in electrochemical performance. To address this challenge, MnO_2 is often combined with conductive materials to enhance its performance [35]. Two-dimensional nanomaterials have emerged as promising electrode materials owing to their unique layered structures and large lateral dimensions [36].

The high surface-to-volume ratio of these materials provides abundant accessible active sites, which can significantly enhance interfacial electrochemical reactions and facilitate efficient charge transfer. Moreover, their high electrical conductivity and tuneable electronic properties, together with versatile surface chemistry, enable tailored electrochemical behaviour and make two-dimensional nanomaterials highly suitable for electrode modification. Transition-metal carbides (MXenes) are an emerging class of two-dimensional materials with unique structural and electrochemical properties [37]. MXenes are characterized by the general formula $M_{n+1}X_nT_x$ (n = 1 to 3), where M represents a transition metal from the early groups, X signifies carbon and/or nitrogen and T_x refers to surface functional groups such as -OH, -O and/or -F [38]. Among them, $Ti_3C_2T_X$ is one of the most extensively studied MXenes due to its excellent electrical conductivity, large surface area, versatile electrochemical properties, and inherent hydrophilicity. Its hydrophilic nature, arising from surface functional groups, facilitates interactions with aqueous solutions and analyte compounds, enhancing sensitivity and charge transfer efficiency. $Ti_3C_2T_X$ has shown great potential in a wide range of applications, particularly in electrochemical sensors and energy storage systems such as supercapacitors and batteries [39]. In this context, the combination of $Ti_3C_2T_X$ MXene nanosheets with MnO_2 nanostructures can create a synergistic composite structure, simultaneously utilize the advantages of both materials and play a crucial role in the design of an efficient electrochemical sensor.

In the present work, a novel and simple modified electrode was designed for the efficient voltammetric determination of dasatinib. For the preparation of this modified electrode, the suspension of the $Ti_3C_2T_X$ MXene nanosheets (NSs)/α-MnO_2 nanorods (NRs) composite was dropped onto the surface of a disposable carbon screen-printed electrode (CSPE). The Ti_3C_2TX MXene NSs/α-MnO_2 NRs composite coated on the CSPE surface enhances conductivity and electroactive sites for dasatinib oxidation, considerably improving sensor performance. Quantitative determination of dasatinib was conducted on the $Ti_3C_2T_X$ MXene NSs/α-MnO_2 NRs/CSPE in the concentration range of 0.01 to 400.0 µM. The value of the limit of detection (LOD) was determined to be 0.005 µM. Finally, a further electrochemical investigation was conducted to assess the performance of the designed sensor for dasatinib determination in the tablet sample, yielding satisfactory results.

Materials and methods

Materials and reagents

The materials and reagents, including manganese(II) sulphate monohydrate ($MnSO_4 \cdot H_2O$), potassium permanganate ($KMnO_4$), sulfuric acid (H_2SO_4), dimethyl sulfoxide (DMSO), dasatinib, sodium hydroxide (NaOH), phosphoric acid (H_3PO_4) and other chemicals, were of analytical grade and obtained from Merck and Sigma-Aldrich. The $Ti_3C_2T_X$ MXene NSs were purchased from Redoxkala (Iran). Phosphate buffer (PB) was used as a supporting electrolyte.

For all electrochemical studies and measurements, a Metrohm Autolab PGSTAT302N potentiostat-galvanostat (The Netherlands), connected to a computer and operated via GPES software for data acquisition, was used. Carbon screen-printed electrodes (CSPEs; Metrohm-DropSens, Spain, ref. 110) were employed in the electrochemical experiments.

Synthesis of $Ti_3C_2T_X$ MXene nanosheets/α-MnO_2 nanorods composite

α-MnO_2 NRs were synthesized using a previously reported method by Rajendiran *et al.* [40]. Firstly, 3.165 g of $MnSO_4.H_2O$ and 1.780 g of $KMnO_4$ were dissolved in 55.0 mL of distilled water with magnetic stirring for 20 min. Then, a certain volume of H_2SO_4 (98 %) was added dropwise to the above solution under magnetic stirring. The final solution was vigorously stirred for approximately 30 min and subsequently transferred to a Teflon-lined autoclave, sealed, and heated to 150 °C for 10 h. After the hydrothermal reaction, the precipitate at the bottom of the autoclave was collected, washed several times with ethanol and distilled water and dried (60 °C for 12 h). Finally, the α-MnO_2 NRs were obtained by annealing the dried precipitate at 400 °C for 5 h in air, with a heating rate of 5 °C min^{-1}.

To prepare the $Ti_3C_2T_X$ MXene NSs/α-MnO_2 NRs composite, $Ti_3C_2T_X$ MXene powder (0.06 g) was first added to 80 mL of DMSO and dispersed to form a homogeneous suspension. After achieving adequate dispersion, prepared α-MnO_2 NRs (0.06 g) were slowly added to the above suspension under constant stirring, which was maintained for 1 h. The suspension was then exposed to ultrasonic irradiation for 2 h to promote better dispersion. Then, the resulting precipitate was separated and washed several times using ethanol and distilled water. The final composite material was obtained after drying the product at 60 °C for 24 h.

Modification of carbon screen-printed electrode surface using the as-prepared $Ti_3C_2T_X$ MXene nanosheets/α-MnO_2 nanorods composite

Initially, 2.0 mg of the prepared $Ti_3C_2T_X$ MXene NSs/α-MnO_2 NRs composite was dispersed in 2.0 mL of deionized water and ultrasonicated for about 30 min to form a homogeneous suspension prior to electrode modification. Subsequently, the surfaces of CSPEs were modified by drop-casting 4.0 µL of this suspension and allowed to dry at ambient temperature.

Results and discussion

Cyclic voltammetry of dasatinib at the surface of bare and modified carbon screen-printed electrode

For the pH optimization studies, cyclic voltammetry (CV) responses of $Ti_3C_2T_X$ MXene NSs/α-MnO_2 NRs/CSPE sensor toward 15.0 µM dasatinib were recorded in PB with various pH values (3.0 to 9.0). From the performed CV measurements, the I_p of dasatinib increases when the pH of PB increases from 3.0 to 7.0, reaches a maximum value at pH 7.0 and then decreases for higher pH values. Consequently, 0.1 M PB at pH 7.0 was employed in all subsequent experiments.

To assess the effectiveness of the prepared $Ti_3C_2T_X$ MXene NSs/α-MnO_2 NRs composite as an electrode material for the voltammetric determination of dasatinib, CV experiments were performed in 0.1 M PB at pH 7.0 containing 100.0 µM dasatinib. The CVs of bare CSPE and $Ti_3C_2T_X$ MXene NSs/α-MnO_2 NRs/CSPE are displayed in Figure 1. A comparison of the recorded CVs showed that Ti_3C_2TX MXene NSs/α-MnO_2 NRs/CSPE exhibited a significantly enhanced CV response toward dasatinib oxidation, with an increased anodic peak current (I_p) of 11.1 µA and a reduced anodic peak potential (E_p) of 790 mV. This improvement likely results from the enlarged effective surface area and increased number of electroactive sites, along with enhanced electron-transfer efficiency and the high electrocatalytic activity of the modified CSPE.

(cc) BY

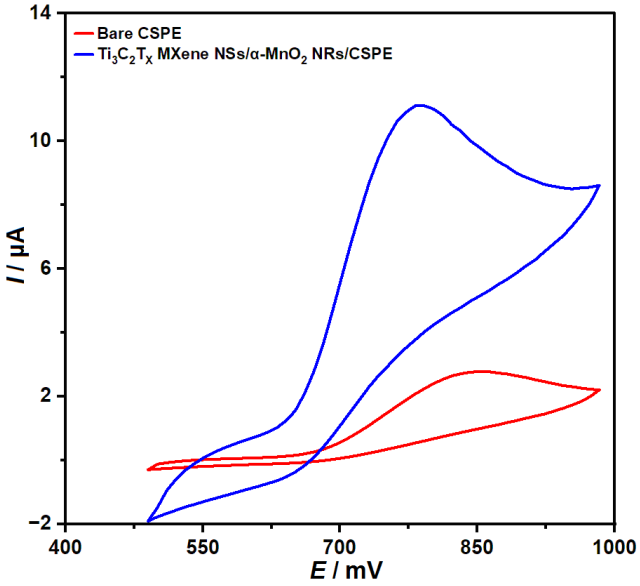


Figure 1. CVs recorded at the bare CSPE (red curve) and $Ti_3C_2T_X$ MXene NSs/α-MnO_2 NRs/CSPE (blue curve) in 0.1 M PB at pH 7.0 containing 100.0 µM dasatinib; scan rate: 50 mV s^{-1}

Influence of scan rate

Cyclic voltammograms from the oxidation of 100.0 µM dasatinib in 0.1 M PB at pH 7.0 were recorded at the $Ti_3C_2T_X$ MXene NSs/α-MnO_2 NRs/CSPE electrode by changing the scan rate from 5 to 300 mV s^{-1}, as illustrated in Figure 2. According to the recorded CV responses, an increase in the *I* of dasatinib was observed with increasing the scan rate. Furthermore, a linear dependence of *I vs*. the square root of the scan rate ($\nu^{1/2}$) plot (Figure 2, inset) indicates that the dasatinib oxidation occurs via a diffusion-controlled process.

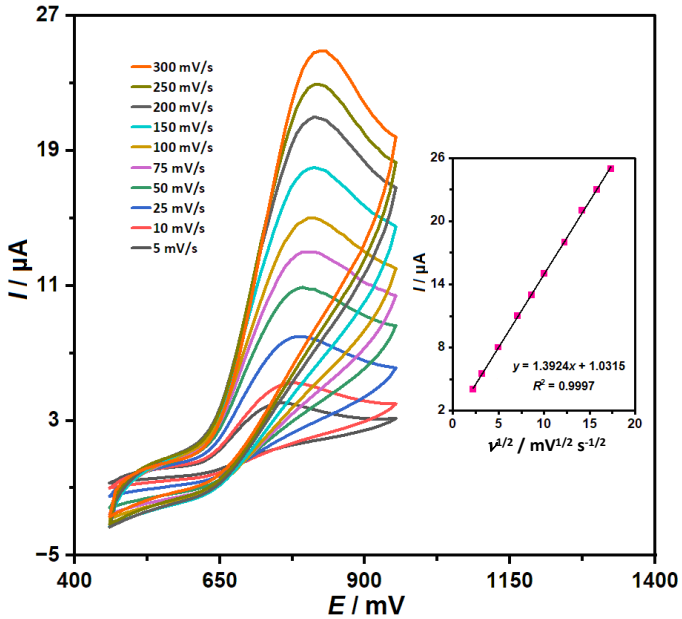


Figure 2. CVs of $Ti_3C_2T_X$ MXene NSs/α-MnO_2 NRs/CSPE in 0.1 M PB at pH 7.0 containing 100.0 µM dasatinib, recorded at different scan rates (5 to 300 mV s^{-1}). Inset: linear plot of I_p *vs.* $\nu^{1/2}$

Chronoamperometric studies

Since the electrochemical oxidation of dasatinib is a diffusion-controlled process, the chronoamperometry method was used to calculate the diffusion coefficient (*D*) of dasatinib at the $Ti_3C_2T_X$ MXene NSs/α-MnO_2 NRs/CSPE surface by applying a step potential of 0.83 V to the working electrode. The resulting current (*I*) *vs.* time (*t*) curves (chronoamperograms) in 0.1 M PB at pH 7.0 containing dasatinib at different concentrations are

presented in Figure 3. For each chronoamperogram obtained at varying concentrations, the *I vs.* $t^{-1/2}$ curves were plotted, showing a linear correlation in all cases (Figure 3A). The slopes derived from the linear fits were then plotted against the corresponding dasatinib concentrations, and the resulting linear curve is presented in Figure 3B. The diffusion coefficient (*D*) of dasatinib was finally calculated to be 3.7×10^{-6} cm^2 s^{-1}, derived from the slope of the linear curve in Figure 3B, using the Cottrell equation for a diffusion-controlled mechanism.

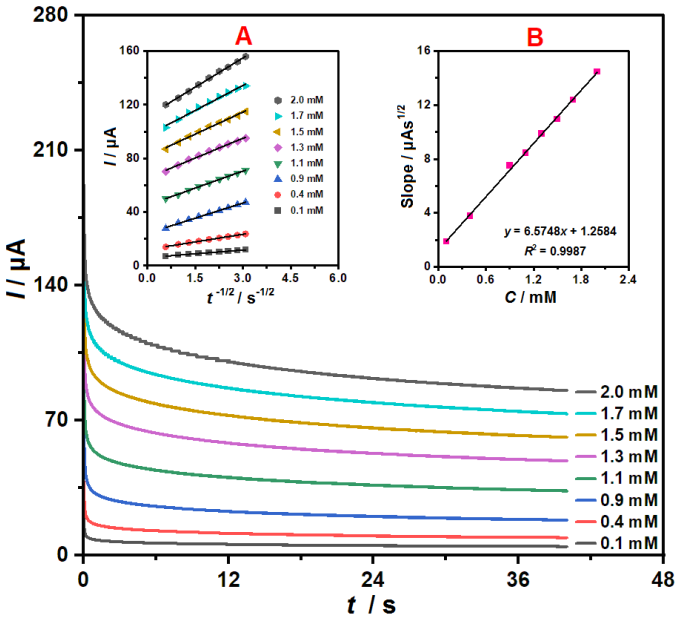


Figure 3. Chronoamperograms obtained at the $Ti_3C_2T_X$ MXene NSs/α-MnO_2 NRs/CSPE in 0.1 M PB at pH 7.0 in the presence of dasatinib with various concentrations (0.1 to 2.0 mM), recorded at a step potential of 0.83 V. Extracted linear dependence between *I* and $t^{-1/2}$ from the chronoamperometric responses (Inset A); plot of the corresponding slopes *vs.* the concentrations of dasatinib (Inset B).

Differential pulse voltammetry measurement of various concentrations of dasatinib

Differential pulse voltammetry (DPV) was used as an electrochemical method with high sensitivity for the quantitative measurements of dasatinib. Therefore, the DPV responses of the $Ti_3C_2T_X$ MXene NSs/α-MnO_2 NRs/CSPE platform were recorded at various concentrations of dasatinib in 0.1 M PB at pH 7.0. The resulting DPV responses can be seen in Figure 4.

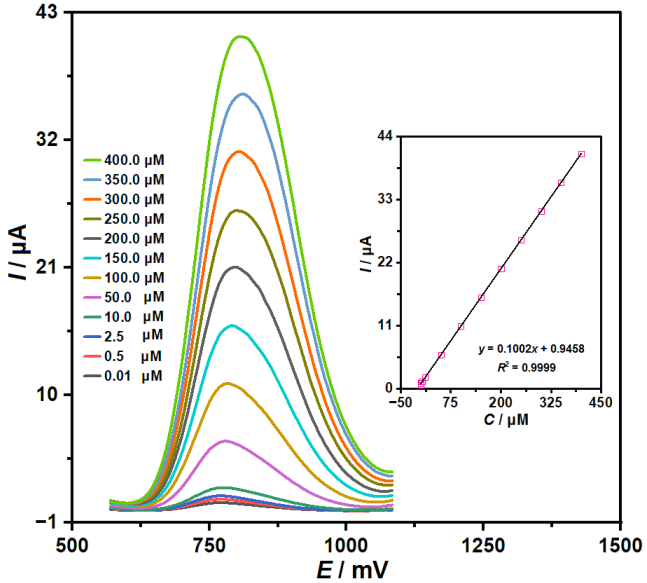


Figure 4. DPVs recorded at the $Ti_3C_2T_X$ MXene NSs/α-MnO_2 NRs/CSPE platform in 0.1 M PB at pH 7.0 containing different concentrations of dasatinib (0.01 to 400.0 µM). Calibration plot for dasatinib determination (Inset)

CC BY

The resulting voltammograms show that the peak currents for dasatinib oxidation increased proportionally with concentration. Moreover, the DPVs showed a linear increase in Ipa with increasing dasatinib concentration, ranging from 0.01 to 400.0 µM, as shown in the calibration plot (Figure 4, Inset). Based on the results, the designed platform showed an excellent analytical response. In the concentration range of 0.01 to 400.0 µM, the designed platform showed high sensitivity (0.1002 µA μM^{-1}). Furthermore, the sensor achieved an LOD of 0.005 µM for dasatinib, demonstrating its ability to detect low concentrations.

Evaluation of the designed sensor for pharmaceutical applications

Furthermore, the practical applicability of the $Ti_3C_2T_X$ MXene NSs/α-MnO_2 NRs/CSPE electrochemical sensor was tested by determining the concentration of dasatinib in prepared solutions of non-spiked and spiked tablet samples. The DPV responses of the sensor for non-spiked and spiked tablet solutions containing different concentrations of dasatinib were recorded. The results for the non-spiked tablet sample showed good agreement between the determined and expected dasatinib concentrations (Table 1), indicating that the tablet matrix did not significantly interfere with the current response. Furthermore, as can be observed in Table 1, the recoveries of the analysed spiked tablet samples ranged from 96.6 to 103.8 %. Therefore, these results indicate that the designed sensing platform is validated and reliable for measuring the target compound in pharmaceutical samples.

Table 1. Results of dasatinib analysis in tablet sample obtained using the $Ti_3C_2T_X$ MXene NSs/α-MnO_2 NRs/CSPE sensing platform

Amount of dasatinib, µM		Recovery, %	RSD, %
Added	Found		
0	3.9	-	3.5
1.0	5.0	102.0	2.1
2.0	5.7	96.6	1.7
3.0	6.8	98.5	2.9
4.0	8.2	103.8	2.4

Conclusions

In summary, the possibility of the voltammetric determination of dasatinib using the $Ti_3C_2T_X$ MXene NSs/α-MnO_2 NRs composite-modified CSPE sensing platform was demonstrated. The results show that the prepared Ti_3C_2TX MXene NSs/α-MnO_2 NRs composite substantially enhanced the sensor's performance for dasatinib determination due to the synergistic effects of its components. The $Ti_3C_2T_X$ MXene NSs/α-MnO_2 NRs/CSPE sensing platform showed good analytical performance for DPV determination of dasatinib, with a broad linear concentration range from 0.01 to 400.0 µM and a low LOD of 0.005 µM. In addition to its good performance, the successful response of the modified CSPE in the analysis of a dasatinib tablet sample demonstrates the feasibility of the designed sensing platform for efficient drug quality control.

Acknowledgments: *This project received financial support from the National Institute for Medical Research Development (NIMAD), Islamic Republic of Iran (grant number 4040284). The authors gratefully acknowledge the Afzalipour Research Institute (ARI).*

Declaration of competing interests: *The authors have no declaration of interest.*

Data availability statement: *The data presented in this study are available on request from the corresponding authors.*

Conflicts of interest: *The authors declare no conflict of interest.*

References

[1] M. Xu, X. Han, H. Xiong, Y. Gao, B. Xu, G. Zhu, J. Li. Cancer nanomedicine: emerging strategies and therapeutic potentials. *Molecules* **28** (2023) 5145. https://doi.org/10.3390/molecules28135145

[2] G. Wei, Y. Wang, G. Yang, Y. Wang, R. Ju. Recent progress in nanomedicine for enhanced cancer chemotherapy. *Theranostics* **11** (2021) 6370-6392. https://doi.org/10.7150/thno.57828

[3] V. Schirrmacher. From chemotherapy to biological therapy: A review of novel concepts to reduce the side effects of systemic cancer treatment. *International Journal of Oncology* **54** (2019) 407-419. https://doi.org/10.3892/ijo.2018.4661

[4] F. M. Zahed, B. Hatamluyi, M. K. Bojdi. A novel electrochemical sensor based on $CuCo_2O_4$/NCNTs modified glassy carbon electrode for simultaneous determination of 6-thioguanine and dasatinib in biological samples. *Journal of Molecular Liquids* **434** (2025) 127889. https://doi.org/10.1016/j.molliq.2025.127889

[5] Y. S. R. V. Jogarao, P. Bharath, Siva V. Ramakrishna, D. Ramachandran. Development & validation of RPHPLC method for quantitative estimation of dasatinib and its impurities in pharmaceutical dosage form. *Journal of Pharmaceutical Research International* **34** (2022) 52-65. https://doi.org/10.9734/jpri/2022/v34i25A35950

[6] Fauziya, A. Gupta, A. Nadaf, S. Ahmad, N. Hasan, M. Imran, A. Sahebkar, G.K. Jain, P. Kesharwani, F.J. Ahmad. Dasatinib: a potential tyrosine kinase inhibitor to fight against multiple cancer malignancies. *Medical Oncology* **40** (2023) 173. https://doi.org/10.1007/s12032-023-02018-5

[7] H. W. Darwish, A. H. Bakheit. Micellar enhanced synchronous spectrofluorimetric method for determination of dasatinib in tablets, human plasma and urine: application to in vitro drug release and content uniformity test. *RSC Aadvances* **5** (2015) 54471-54480. https://doi.org/10.1039/c5ra06795b

[8] A. G. Gonzalez, L. Taraba, J. Hraníèek, P. Kozlík, P. Coufal. Determination of dasatinib in the tablet dosage form by ultra high performance liquid chromatography, capillary zone electrophoresis, and sequential injection analysis. *Journal of Separation Science* **40** (2017) 400-406. https://doi.org/10.1002/jssc.201600950

[9] C. Wen, Q. Zhang, Y. He, M. Deng, X. Wang, J. Ma. Gradient elution LC-MS determination of dasatinib in rat plasma and its pharmacokinetic study. *Acta Chromatographica* **27** (2015) 81-91. https://doi.org/10.1556/achrom.27.2015.1.7

[10] N. A. Lankheet, M. J. Hillebrand, H. Rosing, J. H. Schellens, J. H. Beijnen, A. D. Huitema. Method development and validation for the quantification of dasatinib, erlotinib, gefitinib, imatinib, lapatinib, nilotinib, sorafenib and sunitinib in human plasma by liquid chromatography coupled with tandem mass spectrometry. *Biomedical Chromatography* **27** (2013) 466-476. https://doi.org/10.1002/bmc.2814

[11] Y. Yokoyama, E. Nozawa, M. Morita, E. Ishikawa, T. Mori, M. Sakurai, T. Kikuchi, E. Matsuki, R. Yamazaki, K. Kataoka, A. Jibiki, H. Kawazoe, S. Suzuki, T. Nakamura. Simultaneous quantification of dasatinib, nilotinib, bosutinib, and ponatinib using high-performance liquid chromatography - Photodiode array detection, *Journal of Clinical Laboratory Analysis* **36** (2022) e24598. https://doi.org/10.1002/jcla.24598

[12] C. Jenkins, S. B. Luty, J. E. Maxson, C. A. Eide, B. H. Chang, J. W. Tyner, PTPN11 Mutations in JMML Confer Dasatinib Sensitivity in a TNK2-Dependent Manner, *Blood*, **128** (2016) 3154. https://doi.org/10.1182/blood.V128.22.3154.3154

[13] A. Sonone, M. Thakur, R. Agade, K. Wadher, S.S. Trivedi, UV-visible spectroscopic based quantitative estimation of intranasal dasatinib-encapsulated polymeric nanoparticles in simulated nasal fluid, *Transformative Medical Materials* **1** (2026) 100005. https://doi.org/10.1016/j.trmm.2026.100005

[14] J. Petr. Determination of tyrosine kinase inhibitors via capillary electrophoresis with tandem mass spectrometry and online stacking preconcentration. *Pharmaceuticals* **16** (2023) 186. https://doi.org/10.3390/ph16020186

[15] H. Kataoka, T. Saita, Y. Yamamoto, R. Sogawa, S. Kimura, S. Kimura, C. Shimanoe. Development of a specific and sensitive sandwich enzyme-linked immunosorbent assay for the quantification of dasatinib. *Analytical Biochemistry* **678** (2023) 115272. https://doi.org/10.1016/j.ab.2023.115272

(cc) BY

[16] H. Karimi-Maleh, A. A. Ensafi, H. Beitollahi, V. Nasiri, M. A. Khalilzadeh, P. Biparva. Electrocatalytic determination of sulfite using a modified carbon nanotubes paste electrode: application for determination of sulfite in real samples. *Ionics* **18** (2012) 687-694. https://doi.org/10.1007/s11581-011-0654-z

[17] A. N. Solomonenko, E. V. Dorozhko, J. Barek, E. I. Korotkova, V. O. Semin, A. V. Erkovich, N. V. Aseeva. Adsorptive stripping voltammetric determination of carbofuran in food using novel type of modified carbon-based electrode with grafted layers of nickel. *Talanta* **267** (2024) 125116. https://doi.org/10.1016/j.talanta.2023.125116

[18] S. Z. Mohammadi, F. Mousazadeh. Novel strategy for hematoxylin electrochemical quantification based on screen printed electrode modified with graphene-CoS_2 nanocomposite. *Journal of Environmental and Bioanalytical Electrochemistry* **1** (2025) 132139. https://doi.org/10.48309/jebe.2025.507370.1012

[19] P. Mohammadzadeh Jahani, F. Garkani Nejad, R. Zaimbashi, H. Beitollahi, S. Tajik. Cost-effective voltammetric assay based on modified screen printed carbon electrode for determination of 4-aminophenol. *Journal of Applied Organometallic Chemistry* **5** (2025) 112-122. https://doi.org/10.48309/jaoc.2025.505904.1268

[20] F. Garkani Nejad, H. Beitollahi, I. Sheikhshoaie. Graphene oxide–PAMAM nanocomposite and ionic liquid modified carbon paste electrode: An efficient electrochemical sensor for simultaneous determination of catechol and resorcinol. *Diagnostics* **13** (2023) 632. https://doi.org/10.3390/diagnostics13040632

[21] S. Esmaeelzadeh, N. Akbarzadeh-T. Bimetallic nanoparticle of yttrium-copper metal-organic framework (Y-Cu-MOF) as a novel modifier for determination of ascorbic acid. *Advanced Journal of Nanochemistry and Medicine* **1** (2025) 220-232. https://doi.org/10.48309/ajnm.2025.551291.1019

[22] H. Beitollahi, S. Tajik, F. Garkani Nejad, P. Safaee-Mehr. Carboxylic acid-functionalized MWCNTs@$MoSe_2$ nanostructure-modified screen-printed carbon electrode as an efficient electrochemical sensor for methyl parathion detection in the water samples. *Journal of Alloys and Compounds* **1044** (2025) 184468. https://doi.org/10.1016/j.jallcom.2025.184468

[23] A. V. Papavasileiou, N. Antonatos, J. Luxa, L. Dìkanovský, S. Ashtiani, R. L. Fomekong, Z. Sofer. Two-dimensional VSe_2 nanoflakes as a promising sensing electrocatalyst for nitrobenzene determination in water samples. *Electrochimica Acta* **475** (2024) 143653. https://doi.org/10.1016/j.electacta.2023.143653

[24] P. Mohammadzadeh Jahani, S. Tajik, Z. Dourandish. Electrochemical sensor based on Ce-MOF modified screen printed electrode for metronidazole determination. *Chemical Methodologies* **8** (2024) 123-132. https://doi.org/10.48309/CHEMM.2024.431008.1750

[25] R. Razavi. Nanocarriers in medicine: A comprehensive review of advances and applications. *Advanced Journal of Nanochemistry and Medicine* **1** (2025) 183-193. https://doi.org/10.48309/ajnm.2025.535128.1010

[26] H. Beitollahi, F. Garkani Nejad, S. Z. Mohammadi, S. Tajik. A novel electrochemical sensing platform based on Zn-Co ZIFs/GO nanocomposite and ionic liquid for sensitive determination of methotrexate in the presence of calcium folinate. J*ournal of The Electrochemical Society* **172** (2025) 106503. https://doi.org/10.1149/1945-7111/ae09ff

[27] A. Hajializadeh. Voltammetry determination of vitamin B_6 using modified screen printed electrode. *Journal of Environmental and Bioanalytical Electrochemistry* **1** (2025) 112122. https://doi.org/10.48309/jebe.2025.505996.1010

[28] A. Bazrafkan, F. Garkani Nejad, R. Zaimbashi, H. Beitollahi. Electrochemical sensing platform based on the synergistic effects of MWCNTs and ZIF-L (Zn, Co) for voltammetric determination of dopamine in the presence of uric acid. *Electrochemistry Communications* **176** (2025) 107928. https://doi.org/10.1016/j.elecom.2025.107928

[29] M. Fazli, N. Akbarzadeh-T. Electrochemical determination of hydrazine using modified glassy carbon electrode. *Journal of Environmental and Bioanalytical Electrochemistry* **1** (2015) 211-220. https://doi.org/10.48309/jebe.2025.527588.1024

[30] M. Adeli Nejad, H. Sarhadi, E. Sarhadi. Bisphenol A: Analysis using modified graphite screen printed electrode as an electrochemical sensor. *Advanced Journal of Nanochemistry and Medicine* **1** (2025) 194-202. https://doi.org/10.48309/ajnm.2025.537230.1013

[31] S. Tajik, P. Shams, H. Beitollahi, F. Garkani Nejad. Electrochemical nanosensor for the simultaneous determination of anticancer drugs epirubicin and topotecan using UiO-66-NH_2/GO nanocomposite modified electrode. *Biosensors* **14** (2024) 229. https://doi.org/10.3390/bios14050229

[32] J. M. George, A. Antony., B. Mathew, Metal oxide nanoparticles in electrochemical sensing and biosensing: a review. *Microchimica Acta* **185** (2018) 358. https://doi.org/10.1007/s00604-018-2894-3

[33] C. Zhu, Q. Wu, F. Yuan, J. Liu, D. Wang, Q. Zhang. Novel electrochemical sensor based on MnO_2 nanowire modified carbon paper electrode for sensitive determination of tetrabromobisphenol A. *Chemosensors* **11** (2023) 482. https://doi.org/10.3390/chemosensors11090482

[34] R.S. Ingole, S.L. Kadam, R. Kamat, J.G. Ok, S.B. Kulkarni. Synthesis and electrochemical characterizations of RGO-decorated MnO_2 nanorods/carbon cloth-based wearable symmetric supercapacitors. *Surfaces and Interfaces* **52** (2024) 104976. https://doi.org/10.1016/j.surfin.2024.104976

[35] E. Khezerloo, F. Hekmat. Sensitive voltammetric determination of rifaximin by electrode modified by nanocomposite of MWCNT/MnO_2/Au NPs. *Diamond and Related Materials* **139** (2023) 110280. https://doi.org/10.1016/j.diamond.2023.110280

[36] P. Forouzandeh, S. C. Pillai. Two-dimensional (2D) electrode materials for supercapacitors. *Materials Today: Proceedings* **41** (2021) 498-505. https://doi.org/10.1016/j.matpr.2020.05.233

[37] M. Pogorielov, K. Smyrnova, S. Kyrylenko, O. Gogotsi, V. Zahorodna, A. Pogrebnjak. MXenes—a new class of two-dimensional materials: structure, properties and potential applications. *Nanomaterials* **11** (2021) 3412. https://doi.org/10.3390/nano11123412

[38] P. A. Rasheed, R. P. Pandey, K. A. Jabbar, K. A. Mahmoud. Platinum nanoparticles/Ti_3C_2Tx (MXene) composite for the effectual electrochemical sensing of Bisphenol A in aqueous media. *Journal of Electroanalytical Chemistry* **880** (2021) 114934. https://doi.org/10.1016/j.jelechem.2020.114934

[39] Z. Li, Y. Guo, H. Yue, X. Gao, S. Huang, X. Zhang, H. Zhang. Electrochemical determination of epinephrine based on Ti_3C_2Tx MXene-reduced graphene oxide/ITO electrode. *Journal of Electroanalytical Chemistry* **895** (2021) 115425. https://doi.org/10.1016/j.jelechem.2021.115425

[40] R. Rajendiran, S. Lingalwar, A. Aravindh, A. Karuppiah, P. Balla, P. K. Seelam, U. Lassi. The role of AgNPs in selective oxidation of benzyl alcohol in vapor phase using morphologically tailored MnO_2 nanorods in the presence of air. *Chemical Engineering Journal* **469** (2023) 144007. https://doi.org/10.1016/j.cej.2023.144007

©2026 by the authors; licensee IAPC, Zagreb, Croatia. This article is an open-access article distributed under the terms and conditions of the Creative Commons Attribution license (http://creativecommons.org/licenses/by/4.0/)